PROCEEDINGS B

rspb.royalsocietypublishing.org

Research

Cite this article: Yant L, Collani S, Puzey J, Levy C, Kramer EM. 2015 Molecular basis for three-dimensional elaboration of the *Aquilegia* petal spur. *Proc. R. Soc. B* **282**: 20142778. http://dx.doi.org/10.1098/rspb.2014.2778

Received: 12 November 2014
Accepted: 13 January 2015

Subject Areas:
developmental biology, evolution, plant science

Keywords:
organ shape, *TCP4*, virus-induced gene silencing, hormones, gene expression, *Aquilegia*

Author for correspondence:
Elena M. Kramer
e-mail: ekramer@oeb.harvard.edu

†Present address: Department of Molecular Biology, Max Planck Institute for Developmental Biology, Tübingen 72076, Germany.
‡Present address: Department of Biology, College of William and Mary, Williamsburg, VA 23185, USA.

Electronic supplementary material is available at http://dx.doi.org/10.1098/rspb.2014.2778 or via http://rspb.royalsocietypublishing.org.

THE ROYAL SOCIETY PUBLISHING

Molecular basis for three-dimensional elaboration of the *Aquilegia* petal spur

Levi Yant, Silvio Collani†, Joshua Puzey‡, Clara Levy and Elena M. Kramer

Department of Organismic and Evolutionary Biology, Harvard University, 16 Divinity Ave., Cambridge, MA 02138, USA

By enforcing specific pollinator interactions, *Aquilegia* petal nectar spurs maintain reproductive isolation between species. Spur development is the result of three-dimensional elaboration from a comparatively two-dimensional primordium. Initiated by localized, oriented cell divisions surrounding the incipient nectary, this process creates a pouch that is extended by anisotropic cell elongation. We hypothesized that the development of this evolutionary novelty could be promoted by non-mutually exclusive factors, including (i) prolonged, KNOX-dependent cell fate indeterminacy, (ii) localized organ sculpting and/or (iii) redeployment of hormone-signalling modules. Using cell division markers to guide transcriptome analysis of microdissected spur tissue, we present candidate mechanisms underlying spur outgrowth. We see dynamic expression of factors controlling cell proliferation and hormone signalling, but no evidence of contribution from indeterminacy factors. Transcriptome dynamics point to a novel recruitment event in which auxin-related factors that normally function at the organ margin were co-opted to this central structure. Functional perturbation of the transition between cell division and expansion reveals an unexpected asymmetric component of spur development. These findings indicate that the production of this three-dimensional form is an example of organ sculpting via localized cell division with novel contributions from hormone signalling, rather than a product of prolonged indeterminacy.

1. Background

Plant developmental studies commonly focus on organ identity. However, the most variable aspects of morphology relate to organ elaboration, a broad class of features downstream of organ identity that include organ fusion, colour, shape and other structural elaborations. We have learned a great deal about the genetic basis of complex lateral organ shape from studies of leaves, but the adaptive significance of leaf shape diversity is often difficult to quantify [1]. On the contrary, variation in petal elaboration has clear adaptive significance linked to pollinator interactions: for example, petals display UV pollinator guides, provide landing platforms, create nectar tubes and mimic female pollinators. All these features are thought to coevolve rapidly with pollinators (reviewed [2]).

Petal nectar spurs are a clear example of extreme petal shape modification and appear to contribute to high speciation rates in the New World clade of the genus *Aquilegia* [3,4]. In *Aquilegia*, punctuated evolution of longer spur lengths correlates with shifts to pollinators possessing longer tongues [5,6]. Early hypotheses suggested that these spurs are produced by the activity of 'meristematic knobs' flanking the petal attachment point [7,8]. On the contrary, a recent study tracking *HISTONE4* expression demonstrated that cell divisions are not localized to the attachment point [9]. Instead, the spur develops in two distinct developmental phases: early cell divisions become concentrated in the area surrounding the nascent spur, producing a nectary cup (Phase I; figure 1*a*). These divisions cease when the spur is still a small fraction of its final length, meaning that highly oriented cell elongation drives the majority of spur growth (Phase II). Variation in this second phase, involving anisotropic cell elongation, is the basis for diversity in spur length across the genus [9].

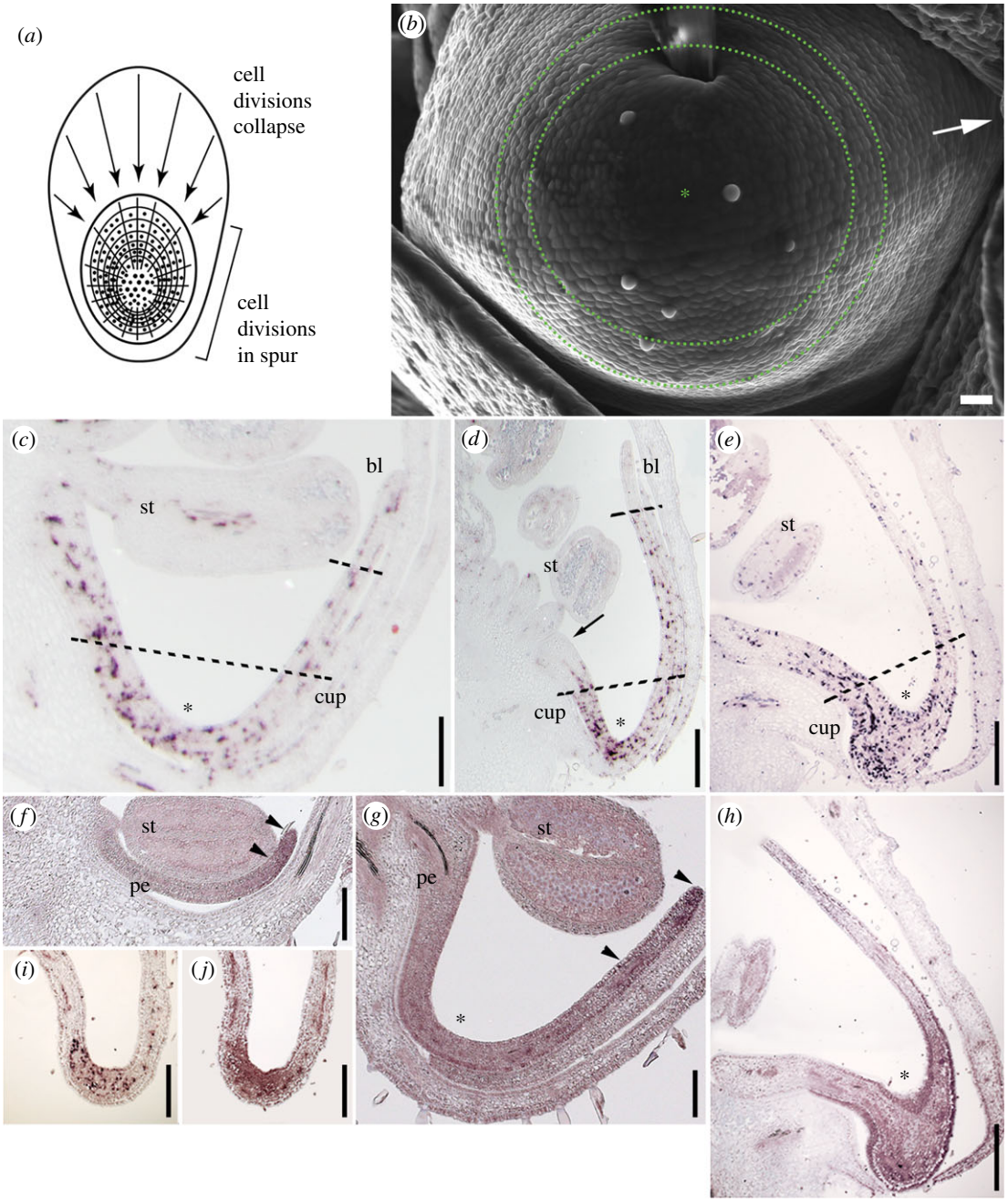

Figure 1. Phase I of *Aquilegia* petal spur development. (*a*) Schematic two-dimensional projection of the spur showing modified cell arrest front with cell divisions localized to the nascent spur (based on [8]). Cell divisions (dots) cease in a wave that progresses circumferentially from the entire margin of the organ towards the presumptive nectary. (*b*) SEM of abaxial surface of 2 mm petal cup. Arrow points to petal attachment point. Zone of tangentially oriented cell walls is highlighted by dotted circles. (*c–e*) *AqHIS4* marking cell division during petal development, which was used as a guide for tissue sampling as indicated by dashed lines. In each panel, asterisks mark the presumptive nectary; st, stamen; bl, blade sample; cup, cup sample. (*c*) Petal primordium from early stage 10 meristem (approx. 1 mm petal). Cell divisions are diffuse throughout the organ but just beginning to decline in the blade region. (*d*) Petal primordium from mid-stage 10 meristem (approx. 3 mm petal). Cell divisions have ceased in the proximal attachment region (arrow) and the distal blade region (bl) but are concentrated in the nascent spur (asterisk). (*e*) Petal primordium from late stage 10 meristem (approx. 5 mm petal). Cell divisions are becoming more concentrated in area surrounding the nectary. (*f–h*) *AqTCP4* expression in early developing petals. In each panel, arrowheads indicate the extent of strongest expression. (*f*) Stamen (st) and petal (pe) primordia in stage 8 floral meristem. (*g*) Stamen (st) and petal (pe) primordia in early stage 10 floral meristem. (*h*) Petal primordium from late stage 10 meristem. (*i–j*) Spur tips from stage 11 meristem. (*i*) *AqHIS4* expression shows that cell divisions have contracted to a domain only marking the nascent nectary. (*j*) Corresponding *AqTCP4* expression overlaps with this domain. Scale bars, 30 µm in *b*, 200 µm in *c*, *f* and *g*, 0.5 mm in *d*, *i* and *j*, and 1 mm in *e* and *h*. (Online version in colour.)

With this framework, we ask the following question: what developmental modules underlie the early phase of spur formation? If we focus just on Phase I, in which cell divisions localize to a specific region, the question centres on how two factors—(i) spatial control of the transition from cell division to expansion and (ii) patterned orientation of new cell walls—direct three-dimensional organ sculpting. One attractive hypothesis is that maintenance of indeterminacy may contribute to petal spur development. Candidate genes for this mechanism include the type I KNOX gene *SHOOTMERISTEMLESS* (*STM*). Many homologues of *STM* play critical roles in the maintenance of the shoot apical meristem (SAM) by promoting cell division and suppressing differentiation [10]. Additionally, in taxa with compound

leaves these genes play similar roles in prolonging indeterminate growth [11]. Two *Antirrhinum* mutants that develop spur-like structures were found to be caused by ectopic expression of homologues of *Arabidopsis STM* [12]. Recently, an investigation of the closely related, spurred genus *Linaria* found that the KNOX orthologues are expressed in petals, including the spur-producing ventral petal [13]. These findings suggest a model that places petal nectar spurs within the context of a broad spectrum of complex lateral organs that use KNOX genes to maintain indeterminacy in order to produce leaflets, lobes and even adventitious meristems (reviewed in [14,15]). While our previous study ruled out the existence of conspicuous 'meristematic knobs', it is still possible that KNOX genes are involved in nascent spur formation and promote a mechanism involving cell fate indeterminacy.

Alternatively, it is possible that genes controlling the late transition between cell proliferation and expansion could generate the extreme curvature of the petal spur without any contributions from the KNOX genes. In both simple and complex lateral organs, interacting genetic modules have been described that regulate laminar curvature (reviewed in [16]). The localization of cell division-promoting proteins, such as the GROWTH-REGULATING FACTORS (GRFs) and their interacting cofactors the GIFs, becomes delimited by division-repressing loci, including members of the *TEOSINTE BRANCHED/CYCLOIDEA/PCF* (*TCP*) transcription factor family. Broadly, these pathways govern the localization and timing of cell divisions as well as the subsequent pattern and orientation of cell elongation. The misregulation of either cell division or cell expansion results in curled, wrinkled or ruffled laminae (e.g. [17–19]). Theoretically, the observed localization of cell divisions in the nascent petal spur [9] could be sufficient to create the outpocketing of the spur cup from the lamina [20]. So, could spur development be simply owing to localized expression of genes that promote cell division in petals?

The broad goal of this study is to identify developmental modules associated with the localized cell divisions seen in the *Aquilegia* spur during its initial outpocketing. We use tissue dissection combined with RNA-seq to identify a number of candidate pathways. We do not detect any contribution from indeterminacy factors such as the type I KNOX transcription factors, but present both expression and functional evidence that localized tissue sculpting plays a critical role. Further, strong evidence for the relocalization of many auxin signalling-related factors suggests a novel role for this hormone in spur development. Together, these findings indicate that the *Aquilegia* petal spur is an example of extreme organ curvature rather than a product of prolonged meristematic indeterminacy.

2. Material and methods

(a) Plant material

Transcriptome sequencing, functional gene knockdown by virus-induced gene silencing (VIGS) and *in situ* hybridization were carried out on *Aquilegia coerulea* L. 'Origami', as previously described [21]. All plants were grown in 14 h photoperiods at 18°C during day and 15°C during night.

(b) RNA-sequencing and analysis

Triplicate pools of the distal 0.5 mm of petal spur cups and blades were removed under a dissecting microscope at three stages over petal spur development and immediately flash frozen in liquid nitrogen (1 mm, 3 mm and 6–7 mm spur length; figure 1*c–e*). For each bioreplicate, we dissected the entire relevant section from each of four to five spurs from a single flower, with separate bioreplicates drawn from different plants. Total RNA was isolated using the Qiagen RNeasy Micro kit (Qiagen, Valencia, CA, USA), including a repeated elution step. Intact RNA (as determined by Agilent Bioanalyzer) was used as input for Illumina TruSeq RNA (Illumina, San Diego, CA, USA) library generation. Residual primers and any primer dimer were eliminated using a second AMPure bead clean-up (Beckman Coulter, Danvers, MA, USA). All libraries were quality confirmed for correct size distributions by Bioanalyzer, quantified by QBIT (Life Technologies, Carlsbad, CA, USA) and quantitative PCR using the SYBR Fast Illumina Library Quantification Kit (Kapa Biosystems, Wilmington, MA, USA) and pooled in order to give equal coverage from each library over multiple HiSeq2000 lanes, using version 2 chemistry. All Illumina data were assessed for basic quality with FastQC v. 0.10.0 (http://www.bioinformatics.babraham.ac.uk/projects/fastqc/). Reads were then trimmed all to a minimum of Q28 with FASTQ Quality Trimmer (FASTX-Toolkit v. 0.0.13; http://hannonlab.cshl.edu) or trimmed to 50 bp, whichever was shorter. Read mapping was performed with TopHat v. 2.0.7, using the Aquilegia195 annotation as reference [22]. Transcripts were assembled for individuals using Cufflinks v. 2.1.1 [23], using default parameters. Resultant files were converted, sorted and indexed with SAMtools v. 0.1.18 (http://samtools.sourceforge.net/). Uniquely mapped reads were counted in 24 823 gene models and converted to count-based data using HTSeq v. 0.5.3 in Python v. 2.7.3 (http://www-huber.embl.de/users/anders/HTSeq). Because counting variance is much higher for lowly expressed transcripts, we excluded all gene models with fewer than an average of 1 cpm in three samples for each blade/cup comparison. We assessed differential expression among the remaining genes using edgeR v. 3.3.8 [24,25] in RStudio v. 0.98.501, using triplicate biological replicates for every tissue and time point.

(c) Identification and isolation of candidate genes

In order to further investigate mRNA expression patterns over time in selected genes, *Aquilegia* homologues of the *Arabidopsis thaliana* KNOX genes *STM* and *KNAT1*, as well as *TCP4*, were identified by using BLAST [26] of the *A. thaliana* nucleotide sequences against the publicly available *Aquilegia coerulea* L. 'Origami' genome sequence [22]. The *Aquilegia* homologue of *HISTONE4* (*HIS4*) has been previously characterized [9]. For *KNOX* genes, nine annotated loci were identified. In two cases, the loci as annotated appeared to represent the separate 5′ and 3′ ends of a single gene. Examination of the genomic locus allowed prediction of contiguous reading frames; thus, a total of seven loci were analysed. For *TCP* genes, 13 annotated loci appear to represent *TCP* family members, but only three of these fall into class I of the *TCP-C* subfamily based on characteristics outlined in [27]. In order to determine the exact orthology of the putative *Aquilegia TCP4* and KNOX loci, we performed phylogenetic analyses using a maximum-likelihood approach as implemented by RAxML in the CIPRES web portal [28–30]. In both cases, amino acid alignments were constructed using conserved domains of gene sequences from multiple core eudicot and monocot taxa. All accession numbers are displayed in electronic supplementary material, figure S2.

(d) *In situ* hybridization

Once orthology was established, fragments of *AqTCP4*, *AqSTM* and *AqKN* were designed that did not include highly conserved domains and were amplified from *A. vulgaris* cDNA using PCR (see electronic supplementary material, table S1 for

primer sequences). Resultant PCR products were cloned using the TOPO-TA Cloning Kit (Life Technologies). Identity and orientation of the inserts was confirmed by sequencing. All *in situ* hybridization steps were conducted as described by Kramer [31]. Results were visualized in the Harvard Center for Biological Imaging on a Zeiss AxioImager Z2 microscope. Developmental floral stages were classified according to Ballerini & Kramer [32] as reported in electronic supplementary material, table S2. The position of the presumptive nectary can be determined by comparing serial sections and identifying the sections that contain the longest extent of the developing spur. Logically, this must represent a radial longitudinal section in which the distal tip is the nascent nectary.

(e) Virus-induced gene silencing

The VIGS inoculation of the TRV2-*AqANS* positive control plasmid was performed as previously described [33,34]. To generate the TRV2-*AqTCP4-AqANS* construct, a 300 bp fragment of *AqTCP4* was amplified with primers that added EcoRI and Xba sites to the respective 5′ and 3′ ends of the PCR product (TCP4_EcoR1: CGGAATTCCGTATCAAGAAGGCAAAGGCTGC, TCP4_Xba 1: CGTCTAGACGAATGGGAAAGAAAGACTTAATGG). This PCR product was used to produce the TRV2-*AqTCP4-AqANS* construct as described by Kramer *et al*. [34]. Four sets of 100–110 *Aquilegia coerulea* 'Origami' plants at the four to six true leaf stage were vernalized at 4°C for four weeks; 1 d after the plants had been removed from vernalization, they were treated as described for seedlings in [33]. Seventy-eight control plants were treated with TRV1 and TRV2-*AqANS*. Flowers showing strong *AqANS* silencing were photo-documented and, on maturation, dissected. Individual organs were photographed using a Canon X type digital SLR camera (Canon, USA). For flowers showing silencing, petals were either frozen at −80°C for subsequent RNA expression analysis or fixed in freshly prepared, ice-cold formalin–acetic acid–alcohol for scanning electron microscopy (SEM) analysis. This process was also repeated for several unsilenced flowers from the TRV2-*AqTCP4-AqANS* cohort, as well as flowers that were treated with TRV2-*AqANS* as controls. SEM analysis and light microscopy was performed as described previously [34].

(f) Expression analysis of virus-induced gene silencing-treated organs

To confirm *AqTCP4* silencing, total RNA was isolated and cDNA was prepared from floral organs as described in [35,36]. qRT-PCR analysis was carried out using PerfeCTa SYBR Green FastMix, Low ROX for qPCR (Quanta BioSciences, Gaithersburg, MD, USA) in a Stratagene (Santa Clara, CA, USA) Mx3005P QPCR System. A list of primers is included in electronic supplementary material, table S1. *AqTCP4* transcript abundance was calculated relative to *AqIPP2* (isopentyl pyrophosphate:dimethylallyl pyrophosphate isomerase) using the ddCt method [37]. Three biological replicates were performed with three technical replicates each.

(g) Scanning electron microscopy analysis

Images of spurs from VIGS-treated plants were obtained on a JEOL JSM-6010 LV SEM. Length and width of cells were manually measured using ImageJ software, and length/width was calculated for each cell. For wild-type, the regions selected for analysis were the blade, mid-spur and nectary cup. TCP4-VIGS spur analysis included the adjoining outgrowth and distal outgrowth regions. Twenty cells were measured in each region.

3. Results

(a) Developmental and molecular characterization of the Phase I petal spur

Previous work [9] defined a model of spur development in which a wave of cell division cessation progresses simultaneously from the entire margin of the organ and moves towards the nascent nectary, promoting a localized bulge that constitutes the first stage of spur development (figure 1*a*). The transition from cell division to expansion that marks Phase I begins when the petal is approximately 1 mm in length, as measured from the petal attachment point to the nascent spur tip, which corresponds to what we have defined as early stage 10 (staging given in electronic supplementary material, table S2; figure 1*c*). Close examination of this early stage 10 spur pocket with SEM reveals a distinct orientation of cell walls around the nascent nectary at the spur tip such that newly formed cell walls are tangentially arranged around the nectary (figure 1*b*). As the petal continues to differentiate throughout stage 10, a progressively narrowing region of cell division becomes restricted to the developing nectar spur (figure 1*d–e*). These cell divisions are last observed as a small crescent of activity in the nascent nectary during early stage 11, when the spur is approximately 7–8 mm in length (figure 1*i*).

In order to begin to assess which genes control this process, we conducted a developmental transcriptome study on microdissected regions of very young petals throughout Phase 1 using RNA-seq. We dissected terminal 4–16 mm^2 tissue sections from regions of the cup and blade of both 1 mm and 3 mm spurs, and also spur tip tissue from 6–7 mm spurs, which are undergoing the transition to rapid anisotropic elongation (denoted by dashed lines in figure 1*c–e*). This sampling covers Phase I from its earliest through late stages and should encompass the entire period during which substantial cell divisions are localized to the spur cup. We aligned an average of 43 million reads from each of three biological replicates for every sample and time point to the 24 823 gene models in the JGI *A. coerulea* genome build [22]. After removing models to which less than half the bioreplicates gave confident mapping, 16 393 genes were included in the differential expression analysis at the 1 mm spur stage and 16 515 at the 3 mm spur stage. Of these, the number of genes that were significantly differentially expressed (DE) between any two tissues or time points was 4008. To determine which genes are consistently DE between the blade and cup regions, we sought the intersection of DE genes from each time point (1 mm stage DE, 653 genes; 3 mm stage DE, 1802 genes; electronic supplementary material, dataset 1). This list consisted of the majority of the DE genes from the early 1 mm contrast, 464 of which remained DE at the 3 mm stage. This reveals retention of programs activated early in spur development, but considerable elaboration and gene expression differentiation at the later stage (we observed approx. 3× the quantity of DE genes at 3 mm compared with 1 mm).

Several trends are evident among the group of genes that continue to be DE at both early stages. First, none of the *Aquilegia* type 1 KNOX homologues come up as DE. Second, the majority of type 1 KNOX loci fail default minimal expression filters for all tissues and time points. Third, we observe many factors governing cellular proliferation and

expansion among the most highly expressed of the consistently DE genes. For instance, the cell division control factors *AqTCP4* and *AqANGUSTIFOLIA3* (*AqAN3*) stand out among the most highly expressed DE genes at both time points in the distal blade margin and spur cup, respectively. *AqTCP4* shows very high expression in both tissues but is significantly higher in the blade at the 1 mm and 3 mm stages. By contrast, *AqAN3* (also known as *GRF-INTERACTING FACTOR1* or *GIF1*), while also highly expressed, is enriched in the spur cup (electronic supplementary material, figure S1). Many GRF homologues that might be expected to partner with *AqAN3* are highly expressed but are not DE between the samples.

In addition to enrichment of *AqAN3* in the early developing cup, our data implicate other candidate processes, with many significant DE genes associated with the hormone auxin (electronic supplementary material, figure S1). We see coordinated regulation of genes responsible for auxin synthesis; for example, downregulation of 3 *YUCCA6* homologues in the cup at both time points while the *Aquilegia CYP71A* homologue, also implicated in auxin synthesis, is highly upregulated in all cup samples. Taking the intersection of DE genes at 1 mm and 3 mm, we note that the highest confidence DE gene in spur cups at both time points (lowest false discovery rate: 5.4×10^{-31} and 7.2×10^{-54}, respectively) is an *Aquilegia* homologue of *STYLISH1*, a transcription factor that regulates auxin biosynthesis [38]. A second *Aquilegia* homologue of *STY* is also DE with enrichment in both cup time points. The two *AqSTY* genes show increasing expression over time in growing spur cups. Genes known to be downstream of both auxin and brassinosteroid (BR) signalling are also DE, including 12 *Aquilegia* homologues of *SAUR* (*SMALL AUXIN UP RNA*), which are upregulated in the latest spur time point (7 mm cups). In addition, several AUXIN RESPONSE FACTOR (ARF) family members show enrichment in the spur cup, particularly *Aquilegia* homologues of *ARF3/ETTIN* and *ARF8*. Both of these genes are very highly expressed in all tissues and time points sampled, but are significantly enriched in the 1 mm cup. In terms of the BR-signalling pathway, one of the most strongly DE genes in the 1 mm cup is the *Aquilegia* homologue of *DWARF4*, a cytochrome P450 that catalyses the flux-determining step in the BR synthesis pathway [39]. The *Aquilegia* homologue of *BEH4*, a member of the *BZR1* family of BR response proteins [40], is also strongly enriched in the 3 mm cup.

(b) *In situ* hybridization confirms RNA-seq results for *AqTCP4* and *Aquilegia* type I KNOX genes

Using orthologue-specific probes (electronic supplementary material, figure S2), we examined the expression of the *Aquilegia* orthologue of the cell division regulator *TCP4*, *AqTCP4*, across all stages of floral development. At later stages, when all floral organs are differentiating, *AqTCP4* expression is most strongly detected in the petals. During stages 8–10, expression is relatively broad but is strongest in the petal margin (figure 1*f–g*). In older petals, the most intense expression moves down into the developing spur (figure 1*h*). Thus, *in situ* detection agrees with the RNA-seq data, showing a dynamic *AqTCP4* expression profile during development, consistent with what has been observed for *TCP4* in *Arabidopsis thaliana* [19]. If the *AqHIS4* and *AqTCP4* expression domains are compared, we see that *AqTCP4* expression is highest in the region where cessation of cell division is under way, such that overlap between *AqTCP4* and *AqHIS4* can be observed (figure 1*e,h*). This is true even until the very last stages of the Phase I/II transition when cell divisions only persist in the presumptive nectary (figure 1*i–j*).

In order to confirm the lack of indeterminacy-mediating class I KNOX gene expression detected by the RNA-seq, we also examined *Aquilegia* homologues of the *Arabidopsis* class I KNOX gene subfamily, which includes the locus *KNAT1/BP* as well as *STM* (electronic supplementary material, figure S2). We observed strong association between *AqHIS4* and *AqSTM1* localization in the SAM and early developing compound leaves, as well as broad *AqKN* expression in young floral buds (electronic supplementary material, figure S3–S5). However, neither *AqSTM1* nor *AqKN* were ever detected at any stage of petal development, including even broader temporal sampling through stage 11 (electronic supplementary material, figures S4–S5), although *AqSTM* could be detected in the developing carpels of the same sections (data not shown).

(c) *AqTCP4* restrains proliferation in a restricted domain of the spur tube

Both our transcriptome and *in situ* expression data suggest that the dynamic expression of cell proliferation regulators is important for spur development. In order to disrupt this functional module, we used VIGS via the Tobacco rattle virus (TRV) system to knock down *AqTCP4* mRNA expression. An approximately 300 bp fragment from the highly variable N-terminal region was used to specifically target *AqTCP4* relative to other TCP family members. *Aquilegia ANTHOCYANIDIN SYNTHASE* (*AqANS*) was simultaneously targeted from the same TRV2 construct in order to visually identify plants exhibiting silencing.

We generated a total of 44 independent plants that displayed silencing in a total of 79 flowers. The majority of these plants also exhibited some *AqANS* silencing in leaves. All observed perturbations of floral morphology affected the petals (figure 2*b–g*). Relative to control petals, *AqTCP4* was downregulated in test petals exhibiting *AqANS* silencing an average of eightfold, as assessed by qRT-PCR (range 7–12-fold). As expected with VIGS, we recovered a range of phenotypes: in 43 flowers the petal phenotype was limited to increased spur curvature, while in 36 flowers we obtained strong silencing with a highly consistent phenotype (figure 2*b–g*). *AqTCP4*-silenced petals exhibited extreme morphological distortions on the side of the spur away from the floral pedicel (white arrowheads in figure 2*c–f*), which we term the distal compartment (figure 2*l–m*). This distortion includes localized ectopic outgrowths, which do not appear to be fully formed *de novo* spurs, as they never show any sign of nectary differentiation that is typical of *Aquilegia* spurs (figure 2*d–f*). Instead, we consider them to be buckles in the lamina owing to over-proliferation in the distal compartment relative to the proximal compartment, which never displayed such outgrowths. Over the course of development, the *AqTCP4*-silenced spurs first bent inward towards the stem (figure 2*b*), but then snapped outward owing to localized distortions in the lamina of the distal compartment (figure 2*c–f*). Furthermore, SEM examination of the epidermis in these outgrowths reveals many small, unexpanded cells, consistent with prolonged cell division (figure 2*g*; electronic

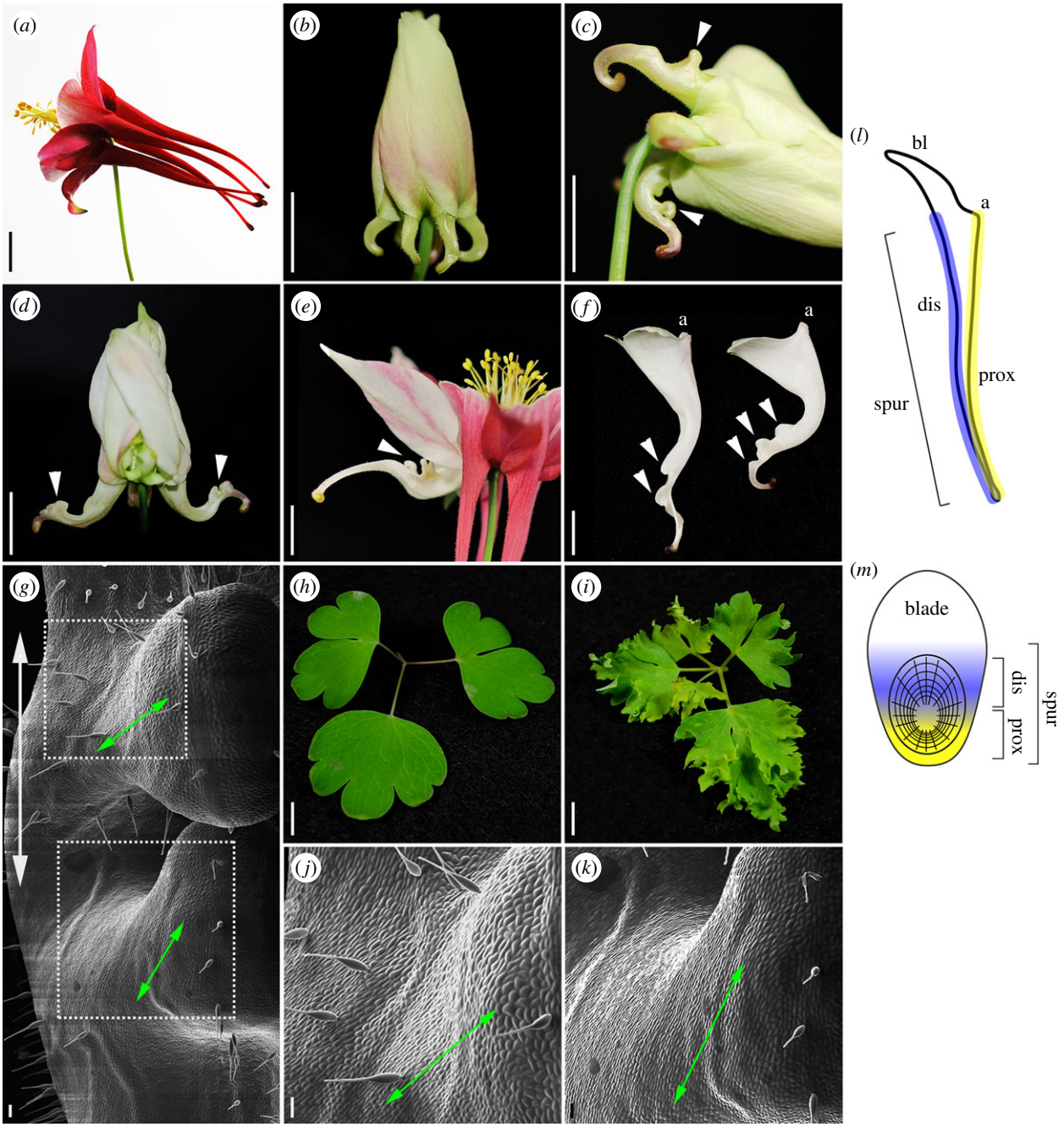

Figure 2. *AqTCP4* functions to restrain cell division in the distal compartment of the spur. (*a*) Untreated *Aquilegia* flower displaying essentially straight petal nectar spurs. (*b–g*) *AqTCP4*-silenced floral phenotypes. Arrowheads point to distal compartment outgrowths. (*b–d*) Strongly silenced flowers at increasing developmental stages (one spur is removed in *d*). Note how spurs bend inward in *b* but then outward in *c* and *d*. (*e*) Flower at anthesis, displaying one silenced spur (white) and four unsilenced (coloured). (*f*) Dissected petal spurs at anthesis displaying excess growth on distal (left) side. (*g,j–k*) SEM of outgrowths, showing reoriented cell files. Primary axis of spur is shown with vertical arrow, angled arrows indicate direction of reorientation of cell files in outgrowth regions. Dashed boxes indicate the higher magnification regions shown in *j* (top box) and *k* (bottom box). (*h*) Unsilenced leaf. (*i*) *AqTCP4*-silenced leaf. (*l*) Mature petal profile indicating blade (bl), spur and attachment point (a), as well as proximal (prox) and distal (dis) compartments. (*m*) Two-dimensional projection of spur in panel *j* showing proximal (prox) and distal (dis) compartments. Scale bars, 1 cm in *a–f* and *h–i*, 100 µm in *g* and *j–k*. (Online version in colour.)

supplementary material, figure S6). SEM analysis also revealed perturbation of both cell orientation and anisotropic expansion in *AqTCP4*-silenced petals (figure 2*g,j–k*; electronic supplementary material, figure S6). In unsilenced petal spurs, Phase I cell walls are tangentially oriented around the nascent nectary (figure 1*a*), a pattern that probably facilitates their later anisotropic expansion along the long axis of the spur. In the buckled regions of *AqTCP4*-silenced spurs, however, cell files are less organized and appear to be reoriented such that they run parallel to the new axis of outgrowth, which is itself perpendicular to the original spur axis (figure 2*g,j–k*). Aside from these phenotypes in the distal compartment of the spur tube, we additionally observed a much higher degree of dissection in the leaf margins of strongly silenced plants (figure 2*i*).

4. Discussion

The production of the three-dimensional nectar spur from the comparatively two-dimensional *Aquilegia* petal primordium begins with cell divisions that progressively become

more localized, collapsing down towards the nascent nectary (figure 1*a*). These oriented cell divisions create a patterned cup that achieves its final size and shape through highly oriented cell elongation [9]. After sampling stages throughout Phase I of spur development, we detected no differential expression of type I KNOX transcripts, of which there are five in *Aquilegia* (electronic supplementary material, figure S1). In fact, the expression of most KNOX homologues across all samples is below default filters for minimal reliable detectable expression using edgeR, and *AqSTM* average raw expression counts are thousands of times lower than those for other major transcription factors. Consistent with this, no expression of either *AqSTM* or *AqKN* was detected using *in situ* hybridization across an even broader range of developmental stages.

As discussed above, KNOX-dependent indeterminacy is not the only way to prolong cell divisions in a lateral organ. Many lateral organs appear to use roughly the same genetic module to control the spatial localization of cell divisions and their eventual cessation [41]. In our case, the single *Aquilegia* ortholog of the cell division suppressor *TCP4* is expressed in the blade margin of 1–3 mm petals, as detected by both RNA-seq and *in situ*, but expression then shifts down into the petal spur at later stages (figure 1*f–h*). In the transition from the 1 mm spur cup to the 3 mm spur cup, we also observe a coordinated repression of 7 *GRFs* (in addition to the GIF *AqAN3*), suggesting orchestrated coregulation as cell divisions decline in this region. This degree of coregulation among homologues of a genetic module primarily known from *Arabidopsis* is notable, given the deep divergence, approximately 120 million years, between *Aquilegia* and *Arabidopsis* [42]. Taken together, these data support the hypothesis that *Aquilegia* petal spurs do not belong to the spectrum of complex lateral organs that use prolonged indeterminacy to generate varied form, but rather are better understood as extreme examples of organ curvature.

Studies in *Arabidopsis* have revealed that *AtTCP4* plays a critical role in regulating petal development, most probably by repressing cell division [43], and modification of *TCP4* homologue expression in petals causes ruffling and curvature in several core eudicot taxa [17,18]. We therefore targeted *AqTCP4* for silencing in order to perturb the relative balance of cell proliferation and expansion, and to determine the effect on the developing petal spur. As confirmation that *AqTCP4* functions in a similar manner to repress cell division in *Aquilegia* lateral organs, we recovered leaf phenotypes that are reminiscent of the *A. thaliana jaw-1D* phenotype, which overexpresses a microRNA that guides messenger RNA cleavage of several *TCP* genes controlling leaf development [19]. While we expected some distortion of spur shape, we unexpectedly discovered that *AqTCP4* plays a specific role in suppressing cell divisions in the distal compartment of the spur; neither the petal blade nor the proximal compartment of the spur are ever effected. This independent development on the two sides of the spur seems surprising in *A. coerulea*, which has essentially straight spurs, but differential elongation has been implicated in other species that naturally have curved spurs (J. Puzey and E. M. Kramer 2012, unpublished data). Thus, our findings indicate that even in species with relatively simple, straight spurs, development of the proximal and distal compartments of the spur can be decoupled, a modularity that could be exploited to create curved spurs in other species. The existence of such modularity does raise another question, however, as to what mechanism is acting in the proximal compartment to regulate the proliferation-to-expansion transition in these cells.

Another intriguing component of the *AqTCP4*-silencing phenotype is the tendency towards reorientation of cell walls in association with the laminar buckles. Together with our examination of wild-type spurs (figure 1*b*), these data suggest that mechanical strain may play an important role in determining cell orientation in the developing spur. It is simple to imagine that during Phase I, proliferating cells in the spur cup experience a circumferential strain that feeds back onto both cytoskeletal organization and other developmental processes, such as auxin trafficking [44,45]. The observed tangential orientation of these cell walls may contribute to both the outpocketing of the spur cup and their proper positioning for the subsequent anisotropic elongation during Phase II. The formation of laminar distortions in the *AqTCP4*-silenced spurs would alter the orientation of this strain and result in comparable shifts in cell orientation. This system may, in fact, provide an excellent model for studying the interplay of mechanical strain, hormone signalling and the genetic pathways governing laminar development.

Our data reveal additional major expression classes associated with the early developing spur pocket. In particular, contingents of coregulated genes that mediate auxin synthesis or response are enriched in the cup at different stages of Phase I. Auxin plays important roles in diverse aspects of organ differentiation, including cell orientation, proliferation and expansion [14]. These loci include auxin biosynthesis genes such as *CYP71A*, as well as downstream factors like *ARF8*, *ARF3/ETT* and *SAUR* genes. The SAUR family has recently been shown to be involved in cellular expansion [46], while *ARF8* influences both cell division and expansion, as well as mediating crosstalk between the BR and auxin pathways [47,48]. Consistent with this, in *Arabidopsis* BR regulates the proximal/distal cell proliferation gradient and the transition to cell expansion [49]. BR signalling is also among the represented processes with, for example, differential expression of *AqBEH4*, a close homologue of BZR1 that mediates BR-induced growth [40], along with *DWF4*, which promotes BR synthesis. On one level, these findings are not surprising, given the highly pleiotropic functions of the auxin pathway and the established role for BR in regulating the transition from cell division to expansion [50]. However, it is important to note that auxin synthesis and peak signalling are most commonly associated with the margins of lateral organs [51], suggesting that the centrally located petal spur represents a novel focal point for auxin responses. The extremely high and differential expression of *Aquilegia STY* homologues in the spur cup is significant in this regard since *Arabidopsis* studies have found these mRNAs to be strongly expressed at the very distal tips of developing organs [52]. Again, this points to a recruitment event in which an auxin-related factor that normally functions at the organ margin has been co-opted for development of a novel, centrally positioned structure. Furthermore, *STY* homologues are primarily known as activators of the YUCCA pathway of auxin synthesis [38], which our RNA-seq indicates is still deployed at the petal margin rather than in the spur. Therefore, it would seem that several aspects of this novel auxin-related focal point are distinct from what is known from core eudicot model systems and may be very recently evolved, given that the nectar spur itself evolved in the common ancestor of the genus *Aquilegia*, around 6 Ma [53].

Data accessibility. All short read data are deposited in the Short Read Archive under BioProject ID PRJNA270946.

Acknowledgements. We thank Kirsten Bomblies and Scott Hodges for helpful discussions, and Florian Jabbour together with one anonymous reviewer for constructive comments on the manuscript.

Author contributions. L.Y. conducted all experiments related to the RNA-seq and VIGS analysis of *AqTCP4*, participated in the design of the study and drafted the manuscript; S.C. conducted the *in situ* hybridization of *AqTCP4*, *AqSTM*, *AqKN* and *AqHIS4*; J.P. participated in the design of the study and conducted SEM analysis of early wild-type spur development; C.L. conducted SEM analysis of wild-type and *AqTCP4*-silenced petal cell morphology; E.M.K. conceived of the study, designed the study, coordinated the study and helped draft the manuscript. All authors gave final approval for publication.

Funding statement. This work was supported by a Ruth L. Kirschstein National Research Service Award from the National Institutes of Health to L.Y. (1F32GM096699) and NSF award IOS-1121005 to E.M.K.

Conflict of interests. The authors have no competing interests relative to this work.

References

1. Nicotra AB, Leigh A, Boyce CK, Jones CS, Niklas KJ, Royer DL, Tsukaya H. 2011 The evolution and functional significance of leaf shape in the angiosperms. *Funct. Plant Biol.* **38**, 535–552. (doi:10.1071/fp11057)
2. Fenster CB, Armbruster WS, Wilson P, Dudash MR, Thomson JD. 2004 Pollination syndromes and floral specialization. *Ann. Rev. Ecol. Evol. Syst.* **35**, 375–403. (doi:10.1146/annurev.ecolsys.34.011802.132347)
3. Hodges SA. 1997 Floral nectar spurs and diversification. *Int. J. Plant Sci.* **158**, S81–S88. (doi:10.1086/297508)
4. Bastida JM, Alcantara JM, Rey PJ, Vargas P, Herrera CM. 2010 Extended phylogeny of *Aquilegia*: the biogeographical and ecological patterns of two simultaneous but contrasting radiations. *Plant Syst. Evol.* **284**, 171–185. (doi:10.1007/s00606-009-0243-z)
5. Whittall JB, Hodges SA. 2007 Pollinator shifts drive increasingly long nectar spurs in columbine flowers. *Nature* **447**, 706–710. (doi:10.1038/nature05857)
6. Hodges SA, Fulton M, Yang JY, Whittall JB. 2004 Verne grant and evolutionary studies of *Aquilegia*. *New Phytol.* **161**, 113–120. (doi:10.1046/j.1469-8137.2003.00950.x)
7. Tepfer SS. 1953 Floral anatomy and ontogeny in *Aquilegia formosa* var. truncata and *Ranunculus repens*. *Univ. CA Publ. Bot.* **25**, 513–648.
8. Tucker SC, Hodges SA. 2005 Floral ontogeny of *Aquilegia*, *Semiaquilegia*, and *Isopyrum* (Ranunculaceae). *Int. J. Plant Sci.* **166**, 557–574. (doi:10.1086/429848)
9. Puzey JR, Gerbode S, Hodges SA, Mahadevan L, Kramer EM. 2012 Evolution of spur-length diversity in *Aquilegia* petals is achieved solely through cell-shape anisotropy. *Proc. R. Soc. B* **279**, 1640–1645. (doi:10.1098/rspb.2011.1873)
10. Barton MK. 2010 Twenty years on: the inner workings of the shoot apical meristem, a developmental dynamo. *Dev. Biol.* **341**, 95–113. (doi:10.1016/j.ydbio.2009.11.029).
11. Koenig D, Sinha N. 2010 Evolution of leaf shape: a pattern emerges. *Curr. Top. Dev. Biol.* **91**, 169–183. (doi:10.1016/s0070-2153(10)91006-5)
12. Golz JF, Keck EJ, Hudson A. 2002 Spontaneous mutations in KNOX genes give rise to a novel floral structure in *Antirrhinum*. *Curr. Biol.* **12**, 515–522. (doi:10.1016/S0960-9822(02)00721-2)
13. Box MS, Dodsworth S, Rudall PJ, Bateman RM, Glover B. 2011 Characterization of *Linaria* KNOX genes suggests a role in petal-spur development. *Plant J.* **68**, 703–714. (doi:10.1111/j.1365-313X.2011.04721.x)
14. Hay A, Tsiantis M. 2010 KNOX genes: versatile regulators of plant development and diversity. *Development* **137**, 3153–3165. (doi:10.1242/dev.030049)
15. Moon J, Hake S. 2011 How a leaf gets its shape. *Curr. Opin. Plant Biol.* **14**, 24–30. (doi:10.1016/j.pbi.2010.08.012)
16. Breuninger H, Lenhard M. 2010 Control of tissue and organ growth in plants. *Curr. Top. Dev. Biol.* **91**, 185–220. (doi:10.1016/s0070-2153(10)91007-7)
17. Koyama T, Ohme-Takagi M, Sato F. 2011 Generation of serrated and wavy petals by inhibition of the activity of TCP transcription factors in *Arabidopsis thaliana*. *Plant Sig. Behav.* **6**, 697–699. (doi:10.4161/psb.6.5.14979)
18. Tanaka Y, Yamamura T, Oshima Y, Mitsuda N, Koyama T, Ohme-Takagi M, Terakawa T. 2011 Creating ruffled flower petals in *Cyclamen persicum* by expression of the chimeric cyclamen TCP repressor. *Plant Biotech.* **28**, 141–147. (doi:10.5511/plantbiotechnology.10.1227a)
19. Palatnik JF, Allen E, Wu XL, Schommer C, Schwab R, Carrington JC, Weigel D. 2003 Control of leaf morphogenesis by microRNAs. *Nature* **425**, 257–263. (doi:10.1038/nature01958)
20. Kennaway R, Coen E, Green A, Bangham A. 2011 Generation of diverse biological forms through combinatorial interactions between tissue polarity and growth. *PLoS Comp. Biol.* **7**, e1002071. (doi:10.1371/journal.pcbi.1002071)
21. Sharma B, Kramer EM. 2013 Virus induced gene silencing in the rapid cycling *Aquilegia coerulea* 'Origami'. In *Virus-induced gene silencing: methods and protocols* (ed. A Becker), pp. 71–81. New York, NY: Springer Science+Business Media.
22. Joint Genome Institute. 2013 Phytozome v9.1. See http://www.phytozome.net.
23. Trapnell C, Williams BA, Pertea G, Mortazavi A, Kwan G, van Baren MJ, Salzberg SL, Wold BJ, Pachter L. 2010 Transcript assembly and quantification by RNA-Seq reveals unannotated transcripts and isoform switching during cell differentiation. *Nat. Biotech.* **28**, 511–515. (doi:10.1038/nbt.1621)
24. Robinson MD, McCarthy DJ, Smyth GK. 2010 edgeR: a bioconductor package for differential expression analysis of digital gene expression data. *Bioinformatics* **26**, 139–140. (doi:10.1093/bioinformatics/btp616)
25. McCarthy DJ, Chen YS, Smyth GK. 2012 Differential expression analysis of multifactor RNA-Seq experiments with respect to biological variation. *Nucleic Acids Res.* **40**, 4288–4297. (doi:10.1093/nar/gks042)
26. Altschul SF, Madden TL, Schaffer AA, Zhang JH, Zhang Z, Miller W, Lipman DJ. 1997 Gapped BLAST and PSI-BLAST: a new generation of protein database search programs. *Nucleic Acids Res.* **25**, 3389–3402. (doi:10.1093/nar/25.17.3389)
27. Navaud O, Dabos P, Carnus E, Tremousaygue D, Herve C. 2007 TCP transcription factors predate the emergence of land plants. *J. Mol. Evol.* **65**, 23–33. (doi:10.1007/s00239-006-0174-z)
28. Stamatakis A, Ott M, Ludwig T. 2005 RAxML-OMP: an efficient program for phylogenetic inference on SMPs. In *8th International Conference on Parallel Computing Technologies* (*PaCT2005*), pp. 288–302. Berlin, Germany: Springer.
29. Stamatakis A, Hoover P, Rougemont J. 2008 A fast bootstraping algorithm for the RAxML web-servers. *Syst. Biol.* **57**, 758–771. (doi:10.1080/106351508 02429642)
30. Miller MA, Holder MT, Vos R, Midford PE, Liebowitz T, Chan L, Hoover P, Warnow T. 2009 The CIPRES Portals. See http://www.phylo.org/sub_sections/portal.
31. Kramer EM. 2005 Methods for studying the evolution of plant reproductive structures: comparative gene expression techniques. In *Molecular evolution: producing the biochemical data* (eds EA Zimmer, EH Roalson), pp. 617–635. San Diego, CA: Elsevier Academic Press.
32. Ballerini ES, Kramer EM. 2011 The control of flowering time in the lower eudicot *Aquilegia formosa*. *EvoDevo* **2**, 4. (doi:10.1186/2041-9139-2-4)
33. Gould B, Kramer EM. 2007 Virus-induced gene silencing as a tool for functional analyses in the emerging model plant *Aquilegia* (columbine, Ranunculaceae). *Plant Meth.* **3**, 6. (doi:10.1186/1746-4811-3-6)
34. Kramer EM, Holappa L, Gould B, Jaramillo MA, Setnikov D, Santiago P. 2007 Elaboration of B gene function to include the identity of novel floral organs in the lower eudicot *Aquilegia* (Ranunculaceae). *Plant Cell* **19**, 750–766. (doi:10.1105/tpc.107.050385)
35. Kramer EM, Di Stilio VS, Schluter P. 2003 Complex patterns of gene duplication in the *APETALA3* and

PISTILLATA lineages of the Ranunculaceae. *Int. J. Plant Sci.* **164**, 1–11. (doi:10.1086/344694)

36. Rasmussen DE, Kramer EM, Zimmer EA. 2009 One size fits all? Molecular evidence for a commonly inherited petal identity program in the Ranunculales. *Am. J. Bot.* **96**, 1–14. (doi:10.3732/ajb.0800038)
37. Livak KJ, Schmittgen TD. 2001 Analysis of relative gene expression data using real-time quantitative PCR and the $2^{-\Delta\Delta C_T}$ method. *Methods* **25**, 402–408. (doi:10.1006/meth.2001.1262)
38. Eklund DM *et al*. 2010 The *Arabidopsis thaliana* STYLISH1 protein acts as a transcriptional activator regulating auxin biosynthesis. *Plant Cell* **22**, 349–363. (doi:10.1105/tpc.108.064816)
39. Choe S. 2007 Signal-transduction pathways toward the regulation of brassinosteroid biosynthesis. *J. Plant Biol.* **50**, 225–229. (doi:10.1007/BF03030649)
40. Yin Y, Vafeados D, Tao Y, Yoshida S, Asami T, Chory J. 2005 A new class of transcription factors mediates brassinosteroid-regulated gene expression in *Arabidopsis*. *Cell* **120**, 249–259. (doi:10.1016/j.cell.2004.11.044)
41. Powell AE, Lenhard M. 2012 Control of organ size in plants. *Curr. Biol.* **22**, R360–R367. (doi:10.1016/j.cub.2012.02.010)
42. Moore MJ, Bell CD, Soltis PS, Soltis DE. 2007 Using plastid genome-scale data to resolve enigmatic relationships among basal angiosperms. *Proc. Natl Acad. Sci. USA* **104**, 19 363–19 368. (doi:10.1073/pnas.0708072104)
43. Nag A, King S, Jack T. 2009 *miR319a* targeting of *TCP4* is critical for petal growth and development in *Arabidopsis*. *Proc. Natl Acad. Sci. USA* **106**, 22 534–22 539. (doi:10.1073/pnas.0908718106)
44. Sampathkumar A, Krupinski P, Wightman R, Milani P, Berquand A, Boudaoud A, Hamant O, Jonsson H, Meyerowitz EM. 2014 Subcellular and supracellular mechanical stress prescribes cytoskeleton behavior in *Arabidopsis* cotyledon pavement cells. *eLife* **3**, e01967. (doi:10.7554/eLife.01967.001)
45. Nakayama N, Smith RS, Mandel T, Robinson S, Kimura S, Boudaoud A, Kuhlemeier C. 2012 Mechanical regulation of auxin-mediated growth. *Curr. Biol.* **22**, 1468–1476. (doi:10.1016/j.cub.2012.06.050)
46. Spartz AK *et al*. 2012 The SAUR19 subfamily of *SMALL AUXIN UP RNA* genes promote cell expansion. *Plant J.* **70**, 978–990. (doi:10.1111/j.1365-313X.2012.04946.x)
47. Jung J-H, Lee M, Park C-M. 2010 A transcriptional feedback loop modulating signaling crosstalks between auxin and brassinosteroid in *Arabidopsis*. *Mol. Cells* **29**, 449–456. (doi:10.1007/s10059-010-0055-6)
48. Varaud E, Brioudes F, Szecsi J, Leroux J, Brown S, Perrot-Rechenmann C, Bendahmane M. 2011 AUXIN RESPONSE FACTOR8 regulates *Arabidopsis* petal growth by interacting with the bHLH Transcription Factor BIGPETALp. *Plant Cell* **23**, 973–983. (doi:10.1105/tpc.110.081653)
49. Gonzalez N *et al*. 2010 Increased leaf size: different means to an end. *Plant Phys.* **153**, 1261–1279. (doi:10.1104/pp.110.156018)
50. Zhiponova MK *et al*. 2013 Brassinosteroid production and signaling differentially control cell division and expansion in the leaf. *New Phyt.* **197**, 490–502. (doi:10.1111/nph.12036)
51. Mattsson J, Sung ZR, Berleth T. 1999 Responses of plant vascular systems to auxin transport inhibition. *Development* **126**, 2979–2991.
52. Eklund DM, Cierlik I, Staldal V, Claes AR, Vestman D, Chandler J, Sundberg E. 2011 Expression of *Arabidopsis* SHORT INTERNODES/STYLISH family genes in auxin biosynthesis zones of aerial organs is dependent on a GCC box-like regulatory element. *Plant Phys.* **157**, 2069–2080. (doi:10.1104/pp.111.182253)
53. Fior S, Li MG, Oxelman B, Viola R, Hodges SA, Ometto L, Varotto C. 2013 Spatiotemporal reconstruction of the *Aquilegia* rapid radiation through next-generation sequencing of rapidly evolving cpDNA regions. *New Phyt.* **198**, 579–592. (doi:10.1111/nph.12163)